

Published in final edited form as:

Biochim Biophys Acta. 2010 July ; 1803(7): 832–839. doi:10.1016/j.bbamcr.2010.03.003.

ErbB4 Regulates the Timely Progression of Late Fetal Lung Development

Washa Liu^{1,#}, Erkhembulgan Purevdorj^{2,#}, Katja Zscheppang², Dietlinde von Mayersbach^{2,3}, Jan Behrens³, Maria-Jantje Brinkhaus⁴, Heber C. Nielsen¹, Andreas Schmiedl³, and Christiane E.L. Dammann^{1,2,*}

¹Division of Newborn Medicine, Floating Hospital for Children at Tufts Medical Center, Boston, MA 02111, USA

²Department of Pediatric Pulmonology and Neonatology, Hannover Medical School, 30625 Hannover, Germany

³Department of Anatomy, Hannover Medical School, 30625 Hannover, Germany

⁴Perinatal Infectious Disease Epidemiology Unit, Hannover Medical School, 30625 Hannover, Germany

Abstract

The ErbB4 receptor has an important function in fetal lung maturation. Deletion of ErbB4 leads to alveolar hypoplasia and hyperreactive airways similar to the changes in bronchopulmonary dysplasia (BPD). BPD is a chronic pulmonary disorder affecting premature infants as a consequence of lung immaturity, lung damage, and abnormal repair. We hypothesized that proper ErbB4 function is needed for the timely progression of fetal lung development. An ErbB4 transgenic cardiac rescue mouse model was used to study the effect of ErbB4 deletion on fetal lung structure, surfactant protein (SP) expression and synthesis, and inflammation. Morphometric analyses revealed a delayed structural development with a significant decrease in saccular size at E18 and more pronounced changes at E17, keeping these lungs in the canalicular stage. SP-B mRNA expression was significantly down regulated at E17 with a subsequent decrease in SP-B protein expression at E18. SP-D protein expression was significantly decreased at E18. Surfactant phospholipid synthesis was significantly decreased on both days, and secretion was down regulated at E18. We conclude that pulmonary ErbB4 deletion results in a structural and functional delay in fetal lung development, indicating a crucial regulatory role of ErbB4 in the timely progression of fetal lung development.

Keywords

Transgenic mice; surfactant; lung structure; inflammation

© 2010 Published by Elsevier B.V.

Corresponding author: Christiane E.L. Dammann, cdammann@tuftsmedicalcenter.org, Fax: 617 636 4233, Phone: 617 636 8738.

[#]Both authors contributed similarly to the manuscript.

Publisher's Disclaimer: This is a PDF file of an unedited manuscript that has been accepted for publication. As a service to our customers we are providing this early version of the manuscript. The manuscript will undergo copyediting, typesetting, and review of the resulting proof before it is published in its final citable form. Please note that during the production process errors may be discovered which could affect the content, and all legal disclaimers that apply to the journal pertain.

Introduction

ErbB receptors play important roles in fetal development [1–4] ErbB receptors are expressed in fetal lung cells [5] and regulate fetal lung maturation via mesenchyme-epithelial cell communication [6, 7]. Their expression in the fetal lung is regulated by a variety of hormones and growth factors [8–10]. The growth factor neuregulin-1, a ligand of ErbB3 and ErbB4 receptors, is secreted by the mature fetal lung fibroblast to stimulate the synthesis of surfactant by lung type II epithelial cells [7]. In the fetal lung, ErbB4 is the most prominent ErbB receptor dimerization partner [5, 11]. Silencing of ErbB4 function using siRNA inhibits fetal surfactant synthesis [12]. ErbB4 knockout mice die at about E11 due to cardiac defects [2]. As in utero death coincides with the onset of lung organogenesis, the role of ErbB receptors in late fetal lung development and maturation needs to be elucidated. HER4^{heart} transgenic mice are rescued from their lethal cardiac defects by expressing the human ErbB4 cDNA under the control of the cardiac-specific myosin (α -MHC) promoter. These animals survive fetal development, can reach adulthood, and are fertile. Adult survivors of homozygote ($-/-$) HER4^{heart} transgenic mice exhibit neural and mammary gland defects [13]. Their lungs show alveolar simplification, airway hyperreactivity, and signs of chronic inflammation [14]. These defects might originate from defective fetal development. Here we present the effects of ErbB4 deletion on late fetal lung development.

Materials and Methods

Materials

Rabbit anti-human surfactant protein (SP) -A, rabbit anti-sheep SP-B, rabbit anti-human pro-SP-C and rabbit anti-mouse SP-D antibodies were from Chemicon Europe (Hofheim, Germany); rabbit polyclonal ErbB4 (C-18) antibody was from Santa Cruz Biotacnology Inc. (Santa Cruz, CA); mouse monoclonal anti-actin clone AC-40 was from Sigma (Hamburg, Germany); goat anti-rabbit IgG (HRP-labelled) and goat anti-mouse IgG (HRP-labelled) were from Zymed Laboratories Inc. (South San Francisco, CA); Precision Plus ProteinTM standards (Dual color) were from Bio-Rad Laboratories (Munich, Germany); Protran nitrocellulose transfer membrane was from Schleicher & Schuell BioScience (Dassel, Germany); Western Lightning Chemiluminescence Reagent Plus (enhanced chemiluminescence, ECL) and methyl [³H]-choline chloride (specific activity 86 Ci/mol) were from Perkin Elmer/Life Sciences (Boston, MA).

HER4^{heart} animals

HER4^{heart} transgenic mice were kindly provided by Carmen Birchmeier in agreement with Martin Gassmann. Animals were housed in the animal facilities of Hannover Medical School and Tufts University under pathogen-free conditions. The animal protocols were approved by the institutional IACUC authorities at both institutions. Animal experiments were performed using fetal E17, and E18 HER4^{heart} mice from heterozygote breedings. Genotyping was performed as previously described [14].

Fibroblast preparation

Pregnant mice were anesthetized, fetuses removed by C-section, and kept in PBS on ice. The E17 fetal lungs were removed, pooled according to genotype $+/+$ and $-/-$, minced into 1mm³ pieces and dissociated in Hanks buffered saline solution (HBSS) containing DNase (20 g/ml) and 0.25% trypsin at 37°C for 10 minutes. The dissociation was stopped by adding DMEM with 10% fetal calf serum (FCS). The cells were filtered through a sterile 45- μ m cell strainer and centrifuged at 650-x g for 10 minutes at 4°C. The cell pellets were resuspended in DMEM with 10% FCS and total cells were plated at 6×10^6 /dish in 100mm² culture dishes for 60 minutes at 37°C to allow for lung fibroblast adherence. The non-adherence

cells were washed away. The fibroblasts were cultured until confluence and analyzed for ErbB4 receptor expression.

Tissue processing

Fetal lungs were obtained and similarly divided into 3 pieces. One part was fixed in 4% PFA, 0.1% GA in 0.2 M HEPES buffer, pH 7.35 for 2 hours, washed with 0.2 M HEPES buffer 6 times for 10 minutes, incubated in sucrose solution overnight at 4°C, and frozen for morphometric and immunohistochemical analyses. The remaining two parts were snap-frozen in liquid nitrogen, stored at -80°C and used for protein and RNA isolation. In additional experiments organotypic lung cultures were prepared from individual fetuses, grown on grids at the air liquid interface and used to study surfactant synthesis and secretion.

Stereological analysis

Stereological analyses were carried out on a Nikon Eclipse 80i microscope (Tokyo, Japan) using the Stereo Investigator Version 6 software (MicroBrightField Inc., Vermont, USA). Three serial hematoxylin-eosin stained cryostat sections (thickness 6 µm, interval 40 µm) from each animal were analyzed using a grid of test points and cycloid lines. Morphometric parameters, including the surface density and volume density of the saccules and their septae, the arithmetic barrier thickness of septae, and the size of the saccules were calculated in E18 lungs. In E17 lungs, the thickness and the volume density of the septal tissue, the volume density of the airspace, the surface density of the saccules or the canalicules, and the size of the saccules or the canalicules were also calculated. This was performed according to the point and intersection counting method [15, 16] as previously described [14].

Western blot of surfactant protein expression

Western blot analyses of frozen fetal lungs for SP-A, SP-B, SP-C and SP-D expression were performed as described previously [14]. Protein expression was quantified by densitometric evaluations for all experiments.

Immunohistochemistry of surfactant proteins

Immunohistochemistry of lung cryosections for SP-A, SP-B, SP-C, and SP-D was performed as described previously [17], with minor modifications. Briefly, 6-µm-thick sections were blocked with 3% H₂O₂/PBS-solution and 5% goat serum, incubated for 15 minutes in an Avidin/Biotin Blocking Kit (SP-2001, Vector Laboratories, Burlingame, USA), and stained with rabbit anti-human surfactant protein (SP) -A, rabbit anti-sheep SP-B, rabbit anti-human pro-SP-C, and rabbit anti-mouse SP-D antibodies (Chemicon Europe, Hofheim, Germany) overnight at 4°C. Staining with the biotin-conjugated affinity purified goat anti-rabbit IgG (Chemicon International Inc. Europe, Hampshire, UK) was followed by incubation in peroxidase-conjugated streptavidin (Jackson ImmunoResearch Europe Ltd., Newmarket, Suffolk, UK) for 30 minutes. Then sections were incubated in DAB (diaminobenzidine) solution for 10 minutes, rinsed in PBS/Tween, dehydrated in ascending series of ethanol, and mounted in Entellan (Entellan Neu, Merck KGaA, Darmstadt, Germany).

Surfactant protein mRNA expression

Real-time PCR for SP-B and SP-D mRNA was performed as previously described [14]. Actin was used as an internal control to normalize the surfactant protein cDNA levels. The relative expression of SP mRNA was calculated using the Ct method. The amount of SP mRNA relative to actin was expressed as $2^{-\Delta Ct}$. Relative SP mRNA expression of

HER4^{heart^{-/-}} animals was compared to the mRNA expression of their litter-specific HER4^{heart^{+/-}} control animals and presented as % of the control values.

Surfactant lipid synthesis (³H-Choline incorporation and secretion)

Fetal lung organotypic cultures were prepared from individual fetuses as previously described [18], cultured in DMEM with 10% fetal bovine serum for 48 hours, and treated with 0.5 Ci/ml ³H-choline for the following 24 hours. The media of the cultures were collected for surfactant lipid secretion analysis. The culture tissue was homogenized and sonicated in ice cold PBS for surfactant lipid incorporation analysis. Aliquots in duplicate were used for protein determination. Following lipid extraction with chloroform and methanol, disaturated phosphatidylcholine (DSPC) was isolated by osmium tetroxide, and separated by thin-layer chromatography on silica gel H chromatography sheets as previously published [7, 12]. The resulting spots were scraped into scintillation fluid, counted in a beta scintillation counter, expressed as disintegrations per minute per g protein, and normalized as percent of experiment-specific controls (HER4^{heart^{+/-}} littermate lungs).

Immunohistochemistry of inflammatory cells

Immunostaining with CD11b antibodies was performed in 6- μ m-thick cryosections as described previously [19]. The procedures and reagents were similar to the immunostaining of surfactant proteins with the exception that the primary antibody was rabbit anti-mouse CD11b (IgG2b, Clone M1/70.15, MorphoSys AbD GmbH, Düsseldorf, Germany; 1:100 in PBS/Tween) antibody. Two to three serial staining sections (interval 40 μ m) were evaluated using a light microscope (Nikon Eclipse 80i fluorescence microscope, Nikon GMBH Duesseldorf, Germany). For each section, 300–400 test fields (size of the test frame: 100 \times 100 μ m) were evaluated with a constant interval of 400 μ m between the test fields in both the x- and y-axis using a stereo investigator system (MicroBrightField, Inc. Williston, Vermont, USA). Cell densities of neutrophils and macrophages were evaluated after counting the CD11b positive cells in the lung parenchyma and were expressed as cell number per mm² (cell density) using the following formula:

$$Q//mm^2 = \frac{\text{number} \times \text{grid size}(400 \times 400\mu\text{m})/\text{test frame}(100 \times 100\mu\text{m})}{\text{area of interest}} \times 1,000,000$$

(Q/=number of counted cells)

Statistics

Data are presented as mean values \pm SEM, if not indicated otherwise. N indicates the number of fetal lungs studied. Statistical significance was considered for p-values <0.05 using the Student's t-test for those data following a normal distribution, and the Mann-Whitney U test otherwise.

Results

ErbB4 expression

We confirmed that E17 HER4^{heart^{-/-}} fibroblasts did not express ErbB4 receptor, while ErbB4 was expressed in HER4^{heart^{+/+}} fibroblasts (Figure 1). The lack of ErbB4 expression in the HER4^{heart^{-/-}} fibroblasts is in agreement with the report of Tidcombe et al who found in this model that ErbB4 mRNA is expressed in only heart and not in other organs such as brain, liver and mammary gland [13]. We have previously reported that ErbB4 is normally expressed in late gestation wild type fetal rat fibroblasts and type II cells and in fetal mouse type II cells and the mouse MLE12 type II cell line [5, 10, 11]. We have also found that

ErbB4 immunostaining is present in fibroblast clusters neighboring developing saccules and in occasional clusters of columnar airway epithelium of late gestation mouse lungs (unpublished data).

Lung morphology

Morphometric analyses of E18 lungs showed a significant decrease in the size of saccules to $91.78 \pm 2.92\%$ ($p=0.04$) in fetal $HER4^{heart-/-}$ lungs ($N=13$) compared to the lungs of their control $HER4^{heart+/-}$ littermates ($N=12$) (Table 1). More dramatic changes were observed at E17 in the lung structure of transgenic mice (Table 2). Most $HER4^{heart-/-}$ lungs corresponded to the canalicular stage of lung development at E17, whereas control lungs had appropriately progressed to the saccular stage (Figure 2A-D). These changes in the $HER4^{heart-/-}$ lungs were confirmed quantitatively. The thickness and the visual volume density of the septal tissue were significantly increased ($122.74 \pm 6.58\%$, $p=0.016$ and $122.23 \pm 3.5\%$, $p<0.001$ respectively), while the volume density of the airspace ($73.71 \pm 3.92\%$, $p<0.001$), and the size of the saccules and canaliculi ($71.77 \pm 3.7\%$, $p<0.001$) were significantly decreased in $HER4^{heart-/-}$ lungs ($N=9$) compared to their $HER4^{heart+/-}$ littermate controls ($N=6$) (Table 2). These results suggested that deletion of ErbB4 simplifies lung structure and delays alveolar development in the late fetal period.

Surfactant protein and mRNA expression

The expression of all four surfactant proteins was analyzed by western blotting and by quantitative real time PCR. At E17, SP-A protein was not changed ($133 \pm 24\%$, $N=7$, $p=0.2$) and SP-A mRNA level was significantly decreased ($50 \pm 5\%$, $N=7$, $p=0.03$) in $HER4^{heart-/-}$ lungs compared to $HER4^{heart+/-}$ control lungs ($100 \pm 3\%$, $N=5$; $100 \pm 22\%$, $N=5$, respectively) (Figure 3A). At E18, SP-A protein expression was not changed ($111 \pm 4\%$, $N=11$, $p=0.15$), but SP-A mRNA was significantly increased ($141 \pm 16\%$, $N=10$, $p=0.03$) compared to $HER4^{heart+/-}$ control lungs ($100 \pm 6\%$, $N=11$; $100 \pm 11\%$, $N=12$, respectively) (Figure 3B). SP-B protein was not changed ($90 \pm 7\%$, $N=12$, $p=0.2$), but SP-B mRNA was significantly decreased ($64 \pm 7\%$, $N=9$, $p=0.04$) at E17 in $HER4^{heart-/-}$ lungs compared to $HER4^{heart+/-}$ control lungs ($100 \pm 4\%$, $N=8$; $100 \pm 13\%$, $N=4$, respectively) (Figure 3C). At E18, SP-B protein was significantly decreased ($76 \pm 7\%$, $N=15$, $p=0.02$), but SP-B mRNA was now normal ($158 \pm 46\%$, $N=14$, $p=0.3$) when compared to $HER4^{heart+/-}$ control lungs ($100 \pm 7\%$, $N=13$; $100 \pm 26\%$, $N=14$, respectively) (Figure 3D). SP-C was not changed at either the protein ($101 \pm 9\%$, $N=12$, $p=0.9$) or mRNA level ($75 \pm 18\%$, $N=10$, $p=0.4$) at E17 in $HER4^{heart-/-}$ lungs compared to $HER4^{heart+/-}$ control lungs ($100 \pm 2\%$, $N=8$; $100 \pm 38\%$, $N=6$, respectively) (Figure 3E). At E18 SP-C was lower at the protein level ($84 \pm 6\%$, $N=12$, $p=0.07$) but higher at the mRNA level ($122 \pm 21\%$, $N=13$, $p=0.6$) compared to $HER4^{heart+/-}$ lungs ($100 \pm 5\%$, $N=8$; $100 \pm 18\%$, $N=14$ respectively) (Figure 3F). However none of these differences were significant. Thus, SP-C was overall not affected in fetal $HER4^{heart-/-}$ mice. At E17, both SP-D protein ($173 \pm 62\%$, $N=7$, $p=0.3$) and SP-D mRNA ($195 \pm 64\%$, $N=8$, $p=0.3$) appeared elevated in $HER4^{heart-/-}$ lungs compared to $HER4^{heart+/-}$ control lungs ($100 \pm 6\%$, $N=5$; $100 \pm 33\%$, $N=6$, respectively). However, these increases did not reach statistical significance (Figure 3G). At E18, SP-D protein was significantly decreased ($78 \pm 6\%$, $N=15$, $p=0.014$), but SP-D mRNA was not changed ($111 \pm 23\%$, $N=13$, $p=0.2$) compared to $HER4^{heart+/-}$ control lungs ($100 \pm 6\%$, $N=13$; $100 \pm 16\%$, $N=12$, respectively) (Figure 3H).

Immunohistochemistry of surfactant proteins

Immunohistochemistry for SP-A, SP-B, SP-C, and SP-D did not show significant differences in the location of surfactant protein expression (data not shown). Staining for SP-B was detected in Clara cells and in developing type II cells of E18 $HER4^{heart+/-}$ (A) and $HER4^{heart-/-}$ (B) fetal lungs (Figure 4).

Surfactant lipid synthesis and secretion

³H-Choline incorporation into disaturated phosphatidylcholine (DSPC), a measure of surfactant phospholipid synthesis, was significantly decreased to 64.7±7.6% (N=4) in E17 HER4^{heart^{-/-}} lungs compared to HER4^{heart^{+/-}} lungs (N=9) (p=0.008) (Figure 5A), and to 50.9±11.5% (N=5) in E18 HER4^{heart^{-/-}} lungs compared to HER4^{heart^{+/-}} lungs (N=14) (p=0.0012) (Figure 5B). Surfactant secretion, measured as ³H-labeled DSPC content in the culture media, was significantly decreased only in E18 HER4^{heart^{-/-}} lungs to 51.6±9.8% (N=5) compared to HER4^{heart^{+/-}} lungs (N=14) (p=0.011), (Figure 5B). At E17 this did not reach statistical significance (HER4^{heart^{-/-}} lungs 65.4±23.6%, N= 4 compare to HER4^{heart^{+/-}} lungs 100±21.8%, N=9, p=0.36) (Figure 5A).

In summary, deletion of ErbB4 disturbs pulmonary surfactant homeostasis by down regulation of SP-B and SP-D expression and surfactant phospholipid synthesis and secretion in the late gestation lung.

Inflammatory cells in the lung

Immunohistochemistry for CD11b showed an increase in inflammatory cells in E17 and E18 HER4^{heart^{-/-}} lungs (Figure 6A). Cell density of CD11b positive cells was significantly increased to 291.2±58.4 (p=0.005) and 47.1±7.6 (p=0.0017) cells/mm² at E17 and E18, respectively in HER4^{heart^{-/-}} lungs (N=7) compared to HER4^{heart^{+/-}} controls (84.3±14.82 and 15.3±2.3 cells/mm² respectively; N=7) (Figures 6B-a,b). This leads to the conclusion that deletion of ErbB4 interferes with the development of the innate pulmonary immune system, triggering a chronic inflammatory response.

Discussion

Pulmonary deletion of ErbB4 resulted in an overall delay in the timely progression of fetal lung development. Delayed structural development was clearly seen in the E17 HER4^{heart^{-/-}} fetal lungs, the stage when the lungs normally advance from the canalicular to the saccular stage. Some catch-up in structural development was observed, as there were less obvious changes in the anatomic structure of the ErbB4-deleted lungs at E18. Since a degree of alveolar simplification persists in the adult HER4^{heart^{-/-}} lungs [14], we speculate that the overall catch-up in progression of lung morphogenesis is not completed at the end of structural lung development in these animals. The murine fetal lung develops morphologically in 4 distinct stages, the pseudoglandular (E9.5-E16.5), the canalicular (E16.5–17.5), the saccular (E17.5-P5) and the alveolar (P5–30) stage [20]. The short duration at the canalicular stage makes the murine model at this gestation very useful for studying the effects of gene deletion on the progression of fetal lung morphogenesis. A similar histological picture is present in fetal mouse lungs lacking tumor necrosis factor- α converting enzyme (TACE). TACE plays a central role in the cleavage and shedding of the ErbB4 ectodomain [21]. Morphologically TACE-deleted animals have immature lungs with decreased lung branching and increased thickness of pulmonary mesenchyme [22], similar to the changes in the ErbB4 deleted lungs, suggesting that the disruption of lung development may be related to an inhibition of ErbB4 function in these animals. Other knock out animal models are known for an arrest in the maturation of the surfactant system at the canalicular stage of lung development, e.g. in mice missing the gene for parathyroid hormone-related protein (PTHrP). Fetal and newborn PTHrP(-/-) lungs show delayed mesenchyme-epithelial interactions leading to an arrested type II cell differentiation and a disrupted development of the pulmonary surfactant system [23]. These similarities in the phenotype in PTHrP and ErbB4 (-/-) lungs are consistent with the observations that ErbB receptor signaling may regulate PTHrP gene expression in various epithelial cells. For example, the epidermal growth factor (EGF) receptor activates PTHrP gene expression in

human keratinocytes [24] and EGF activates PTHrP gene expression in various types of epithelial cells [25, 26].

At E18, the structure of ErbB4-deleted fetal lungs showed evidence of catch-up maturation with progression into the saccular stage. The observation of this catch-up structural development in HER4^{heart-/-} lungs at E18 suggests the activation of compensatory mechanisms to correct for the missing function of ErbB4. Those mechanisms might include the participation of other ErbB receptors. The potential role of compensatory signaling by the remaining ErbB receptors is much more complex than a simple evaluation of receptor protein amounts. Overall baseline expression of the remaining ErbB4 receptors appears unchanged (work in progress), but distinct changes in dimer formation, receptor phosphorylation patterns, specific signaling and receptor fate might be involved. ErbB2 is the ErbB receptor predominantly involved in direct interactions with other proteins [27–29], and would be a likely candidate for involvement in a compensatory process. Other signaling pathways such as the PTHrP pathway, known for its interaction with the EGFR [24–26] might also be involved. Further detailed studies are needed to elucidate these compensatory mechanisms.

Adult HER4^{heart-/-} animals show signs of airway hyperreactivity and an underlying chronic inflammation [14]. This inflammation may have in part contributed to the pulmonary morphometric abnormalities seen in those adult animals. In this study we found that the late gestation fetal lungs already showed increased numbers of inflammatory cells. Based on this, we propose that there is an underlying abnormality in regulation of development of the lung inflammatory system in these ErbB4-deleted lungs.

Fetal ErbB4 deletion led to decreased surfactant phospholipid synthesis and delayed SP-B expression. The normalization of SP-B expression in the adult animals [14] is consistent with the observation that homozygous negative animals can survive without postnatal symptoms of surfactant deficiency and indicates a possible catch-up in the development of the surfactant system in association with the catch-up in morphologic development. In contrast to SP-B deficiency, the persistent change of SP-D protein expression in adulthood (14) may contribute to the increased numbers of inflammatory cells in the fetal lung, demonstrating a role of SP-D in the developmental control of lung immunity [30, 31]. SP-D is a member of the collectin family with immunoregulatory functions [32]. An increased number of inflammatory cells in HER4^{heart-/-} lungs is indicative of abnormal regulation of pulmonary immune development in the ErbB4-deleted lungs. In the fetal lung this led to an upregulation of SP-D mRNA, but not the SP-D protein. This is an obvious disconnect between the protein and RNA level. The upregulation of SP-D mRNA in the fetal lung might be viewed as an attempt to appropriately regulate the development of lung immunity. The reason that the increased SP-D mRNA is not reflected in an increase in protein is not clear. It may reflect a block in transcription or an increased turnover of the protein in the fetal lungs. In adult HER4^{heart-/-} animals, signs of chronic inflammation persist, but SP-D protein and mRNA expression are significantly downregulated [14], suggesting a burn out phenomenon of the RNA upregulation later in life.

Taken together, the findings of affected morphologic development in these animals are similar to a BPD-like picture observed in premature lambs after antenatal exposure to corticosteroids or cytokines [33, 34]. Prenatal inflammation is an important triggering event in the pathogenesis of BPD [35], although the exact mechanisms are unknown. *In vitro* experiments show that glucocorticoid treatment promotes the maturation of the surfactant system (7) and simultaneously changes the expression and dimerization pattern of ErbB receptors in fetal type II cells from a prominent role of ErbB4 towards prominence of ErbB2 signaling [10]. Antenatal glucocorticoid administration improves lung maturation and

prevents RDS in preterm infants [36], but the benefits coincide with an inhibition of alveolar development. The facts that glucocorticoids alter ErbB signaling in fetal lungs and that the anatomic structural changes in the glucocorticoid-treated lungs [33] are similar to those we have identified in fetal and adult ErbB4-deleted lungs [14] suggests that ErbB receptor dysregulation [10] might mediate some of the glucocorticoid effects on developing lung morphogenesis. Reduced branching and increased mesenchymal area around airspaces, as well as disrupted surfactant composition and function in the lungs of HER4^{heart-/-} mice confirms the important role of ErbB4 receptors for the regulation of a timely progression of lung development. Our results suggest that the ErbB4 receptor is critical for a timely transition from the canalicular to saccular stage. This is not surprising since ErbB4 is well known for its role in the timely onset of other maturational processes including puberty [37] and the control of astrogenesis [38]. A loss of ErbB4 function may partially be rescued by compensatory mechanisms that likely include changes in the expression, dimerization patterns and receptor phosphorylation of the other three ErbB receptors. The fact that compensatory mechanisms exist suggests the basic importance of ErbB4 for normal lung development, as evolutionary mechanisms have been developed to compensate for its possible loss. This transgenic ErbB4 mouse model might be useful in studying the pathogenesis and treatment of neonatal lung disease.

Acknowledgments

We would like to thank Drs. M. Gassmann and C. Birchmeier for providing the HER4^{heart} mouse line. We are grateful to C. Acevedo, S. Rozek, and Dr. D. Wedekind for their assistance in animal experiments, breeding and genotyping.

Supported by German Research Foundation (DFG) Grant Da 378/3-1 and Da 378/3-2, Gerber Foundation, Peabody Foundation, Susan B. Saltonstall Funds, and NIH HL-04436 and HL-037930, Tufts Medical Center Institutional Grant.

Abbreviations

BPD	Bronchopulmonary dysplasia
DCt	difference in threshold cycle
DSPC	Disaturated phosphatidylcholine
E	Embryonic day
SP	Surfactant protein
HER4^{heart-/-}	Homozygote ErbB negative transgene
HER4^{heart+/-}	Heterozygote transgene

References

1. Meyer D, Birchmeier C. Multiple essential functions of neuregulin in development. *Nature*. 1995; 378:386–390. [PubMed: 7477375]
2. Gassmann M, Casagrande F, Orioli D, Simon H, Lai C, Klien R, Lemke G. Aberrant neural and cardiac development in mice lacking the ErbB4 neuregulin receptor. *Nature*. 1995; 378:390–394. [PubMed: 7477376]
3. Lee KF, Simon H, Chen H, Bates B, Hung MC, Hauser C. Requirement for neuregulin receptor erbB2 in neural and cardiac development. *Nature*. 1995; 378:394–398. [PubMed: 7477377]
4. Riethmacher D, Sonnenberg-Riethmacher E, Brinkmann V, Yamaai T, Lewin GR, Birchmeier C. Severe neuropathies in mice with targeted mutations in the ErbB3 receptor. *Nature*. 1997; 389:725–730. [PubMed: 9338783]

5. Liu W, Zscheppang K, Murray S, Nielsen HC, Dammann CE. The ErbB4 receptor in fetal rat lung fibroblasts and epithelial type II cells. *Biochim Biophys Acta*. 2007; 1772:737–747. [PubMed: 17553674]
6. Nielsen HC. Epidermal growth factor influences the development clock regulating maturation of the fetal lung fibroblast. *Biochim Biophys Acta*. 1989; 1012:201–206. [PubMed: 2787171]
7. Dammann CE, Nielsen HC, Carraway KL. Role of Neuregulin1 {beta} in the Developing Lung. *Am J Respir Crit Care Med*. 2003; 167:1711–1716. [PubMed: 12663324]
8. Dammann CE, Nielsen HC. Regulation of the epidermal growth factor receptor in fetal rat lung fibroblasts during late gestation. *Endocrinology*. 1998; 139:1671–1677. [PubMed: 9528948]
9. Dammann CE, Ramadurai SR, McCants D, Pham LD, Nielsen HC. Androgen regulation of signaling pathways in late fetal mouse lung development. *Endocrinology*. 2000; 141:2923–2929. [PubMed: 10919280]
10. Dammann CE, Nassimi N, Liu W, Nielsen HC. ErbB receptor regulation by dexamethasone in mouse type II epithelial cells. *Eur Respir J*. 2006; 28:1117–1123. [PubMed: 16899478]
11. Zscheppang K, Korenbaum E, Bueter W, Ramadurai SM, Nielsen HC, Dammann CE. ErbB receptor dimerization, localization, and co-localization in mouse lung type II epithelial cells. *Pediatr Pulmonol*. 2006; 41:1205–1212. [PubMed: 17063476]
12. Zscheppang K, Liu W, Volpe MV, Nielsen HC, Dammann CE. ErbB4 regulates fetal surfactant phospholipid synthesis in primary fetal rat type II cells. *Am J Physiol Lung Cell Mol Physiol*. 2007; 293:L429–L435. [PubMed: 17545485]
13. Tidcombe H, Jackson-Fisher A, Mathers K, Stern DF, Gassmann M, Golding JP. Neural and mammary gland defects in ErbB4 knockout mice genetically rescued from embryonic lethality. *PNAS*. 2003; 100:8281–8286. [PubMed: 12824469]
14. Purevdorj E, Zscheppang K, Hoymann HG, Braun A, von Mayersbach D, Brinkhaus MJ, Schmiedl A, Dammann CE. ErbB4 deletion leads to changes in lung function and structure similar to bronchopulmonary dysplasia. *Am J Physiol Lung Cell Mol Physiol*. 2008; 294:L516–L522. [PubMed: 18203811]
15. Weibel ER. Morphometry of the human lung: the state of the art after two decades. *Bull Eur Physiopathol Respir*. 1979; 15:999–1013. [PubMed: 389332]
16. Bolender RP, Hyde DM, Dehoff RT. Lung morphometry: a new generation of tools and experiments for organ, tissue, cell, and molecular biology. *Am J Physiol*. 1993; 265:L521–L548. [PubMed: 8279570]
17. Schmiedl A, Ochs M, Muhlfeld C, Johnen G, Brasch F. Distribution of surfactant proteins in type II pneumocytes of newborn, 14-day old, and adult rats: an immunoelectron microscopic and stereological study. *Histochem Cell Biol*. 2005:1–12.
18. Amato M, Petit K, Fiore HH, Doyle CA, Frantz ID 3rd, Nielsen HC. Effect of exogenous surfactant on the development of surfactant synthesis in premature rabbit lung. *Pediatr Res*. 2003; 53:671–678. [PubMed: 12612208]
19. Skripuletz T, Schmiedl A, Schade J, Bedoui S, Glaab T, Pabst R, von Horsten S, Stephan M. Dose-dependent recruitment of CD25+ and CD26+ T cells in a novel F344 rat model of asthma. *Am J Physiol Lung Cell Mol Physiol*. 2007; 292:L1564–L1571. [PubMed: 17351063]
20. Warburton D, Schwarz M, Tefft D, Flores-Delgado G, Anderson KD, Cardoso WV. The molecular basis of lung morphogenesis. *Mech Dev*. 2000; 92:55–81. [PubMed: 10704888]
21. Vecchi M, Carpenter G. Constitutive proteolysis of the ErbB-4 receptor tyrosine kinase by a unique, sequential mechanism. *J Cell Biol*. 1997; 139:995–1003. [PubMed: 9362517]
22. Zhao J, Chen H, Peschon JJ, Shi W, Zhang Y, Frank SJ, Warburton D. Pulmonary hypoplasia in mice lacking tumor necrosis factor-alpha converting enzyme indicates an indispensable role for cell surface protein shedding during embryonic lung branching morphogenesis. *Dev Biol*. 2001; 232:204–218. [PubMed: 11254358]
23. Rubin LP, Kovacs CS, De Paepe ME, Tsai SW, Torday JS, Kronenberg HM. Arrested pulmonary alveolar cytodifferentiation and defective surfactant synthesis in mice missing the gene for parathyroid hormone-related protein. *Dev Dyn*. 2004; 230:278–289. [PubMed: 15162506]
24. Cho YM, Lewis DA, Koltz PF, Richard V, Gocken TA, Rosol TJ, Konger RL, Spandau DF, Foley J. Regulation of parathyroid hormone-related protein gene expression by epidermal growth factor-

- family ligands in primary human keratinocytes. *J Endocrinol.* 2004; 181:179–190. [PubMed: 15072578]
25. Heath JK, Southby J, Fukumoto S, O'Keeffe LM, Martin TJ, Gillespie MT. Epidermal growth factor-stimulated parathyroid hormone-related protein expression involves increased gene transcription and mRNA stability. *Biochem J.* 1995; 307(Pt 1):159–167. [PubMed: 7717970]
 26. Ferrari SL, Rizzoli R, Bonjour JP. Effects of epidermal growth factor on parathyroid hormone-related protein production by mammary epithelial cells. *J Bone Miner Res.* 1994; 9:639–644. [PubMed: 8053392]
 27. Eisenberg A, Biener E, Charlier M, Krishnan RV, Djiane J, Herman B, Gertler A. Transactivation of erbB2 by short and long isoforms of leptin receptors. *FEBS Letters.* 2004; 565:139–142. [PubMed: 15135067]
 28. Ray A, Nkhata KJ, Cleary MP. Effects of leptin on human breast cancer cell lines in relationship to estrogen receptor and HER2 status. *Int J Oncol.* 2007; 30:1499–1509. [PubMed: 17487372]
 29. Seton-Rogers SE, Lu Y, Hines LM, Koundinya M, LaBaer J, Muthuswamy SK, Brugge JS. Cooperation of the ErbB2 receptor and transforming growth factor beta in induction of migration and invasion in mammary epithelial cells. *Proc Natl Acad Sci U S A.* 2004; 101:1257–1262. [PubMed: 14739340]
 30. Botas C, Poulain F, Akiyama J, Brown C, Allen L, Goerke J, Clements J, Carlson E, Gillespie AM, Epstein C, Hawgood S. Altered surfactant homeostasis and alveolar type II cell morphology in mice lacking surfactant protein D. *Proc Natl Acad Sci U S A.* 1998; 95:11869–11874. [PubMed: 9751757]
 31. Korfhagen TR, Sheftelyevich V, Burhans MS, Bruno MD, Ross GF, Wert SE, Stahlman MT, Jobe AH, Ikegami M, Whitsett JA, Fisher JH. Surfactant protein-D regulates surfactant phospholipid homeostasis in vivo. *J Biol Chem.* 1998; 273:28438–28443. [PubMed: 9774472]
 32. Wright JR. Immunoregulatory functions of surfactant proteins. *Nat Rev Immunol.* 2005; 5:58–68. [PubMed: 15630429]
 33. Polglase GR, Nitsos I, Jobe AH, Newnham JP, Moss TJ. Maternal and intra-amniotic corticosteroid effects on lung morphometry in preterm lambs. *Pediatr Res.* 2007; 62:32–36. [PubMed: 17515831]
 34. Willet KE, Kramer BW, Kallapur SG, Ikegami M, Newnham JP, Moss TJ, Sly PD, Jobe AH. Intra-amniotic injection of IL-1 induces inflammation and maturation in fetal sheep lung. *Am J Physiol Lung Cell Mol Physiol.* 2002; 282:L411–L420. [PubMed: 11839534]
 35. Jobe AH, Bancalari E. Bronchopulmonary dysplasia. *Am J Respir Crit Care Med.* 2001; 163:1723–1729. [PubMed: 11401896]
 36. Roberts D, Dalziel S. Antenatal corticosteroids for accelerating fetal lung maturation for women at risk of preterm birth. *Cochrane Database Syst Rev.* 2006; 3:CD004454. [PubMed: 16856047]
 37. Prevot V, Rio C, Cho GJ, Lomniczi A, Heger S, Neville CM, Rosenthal NA, Ojeda SR, Corfas G. Normal Female Sexual Development Requires Neuregulin-erbB Receptor Signaling in Hypothalamic Astrocytes. *J. Neurosci.* 2003; 23:230–239. [PubMed: 12514220]
 38. Sardi SP, Murtie J, Koirala S, Patten BA, Corfas G. Presenilin-dependent ErbB4 nuclear signaling regulates the timing of astrogenesis in the developing brain. *Cell.* 2006; 127:185–197. [PubMed: 17018285]

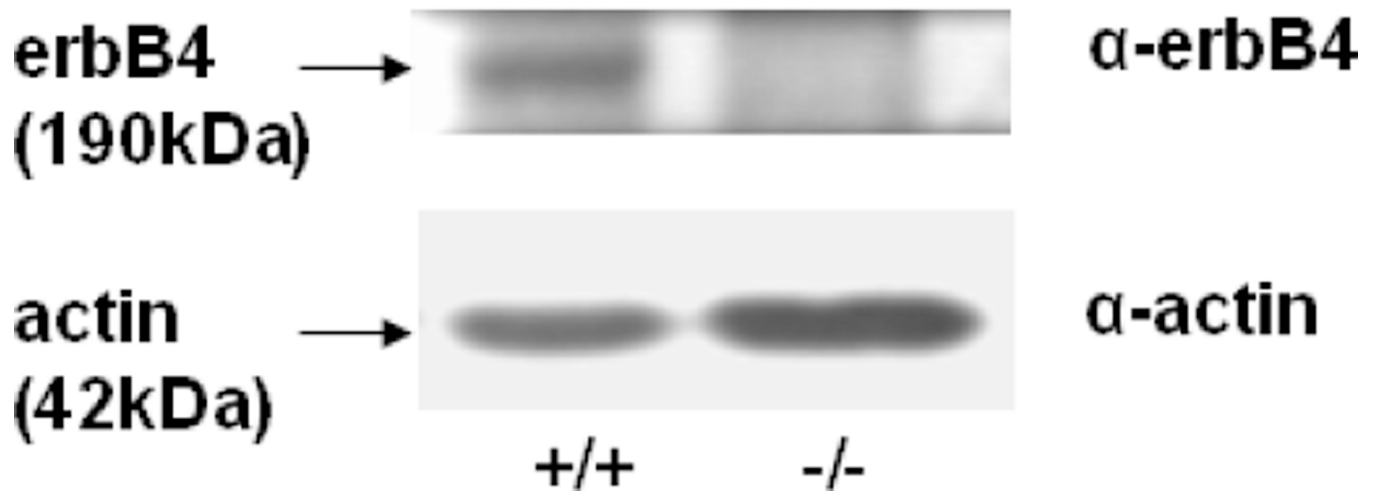


Figure 1. Representative Western blot of ErbB4 expression in freshly isolated primary E17 fibroblasts of $HER4^{heart+/+}$ (left panel) and $HER4^{heart-/-}$ (right panel) lungs, confirming the deletion of ErbB4 in $HER4^{heart-/-}$ lungs.

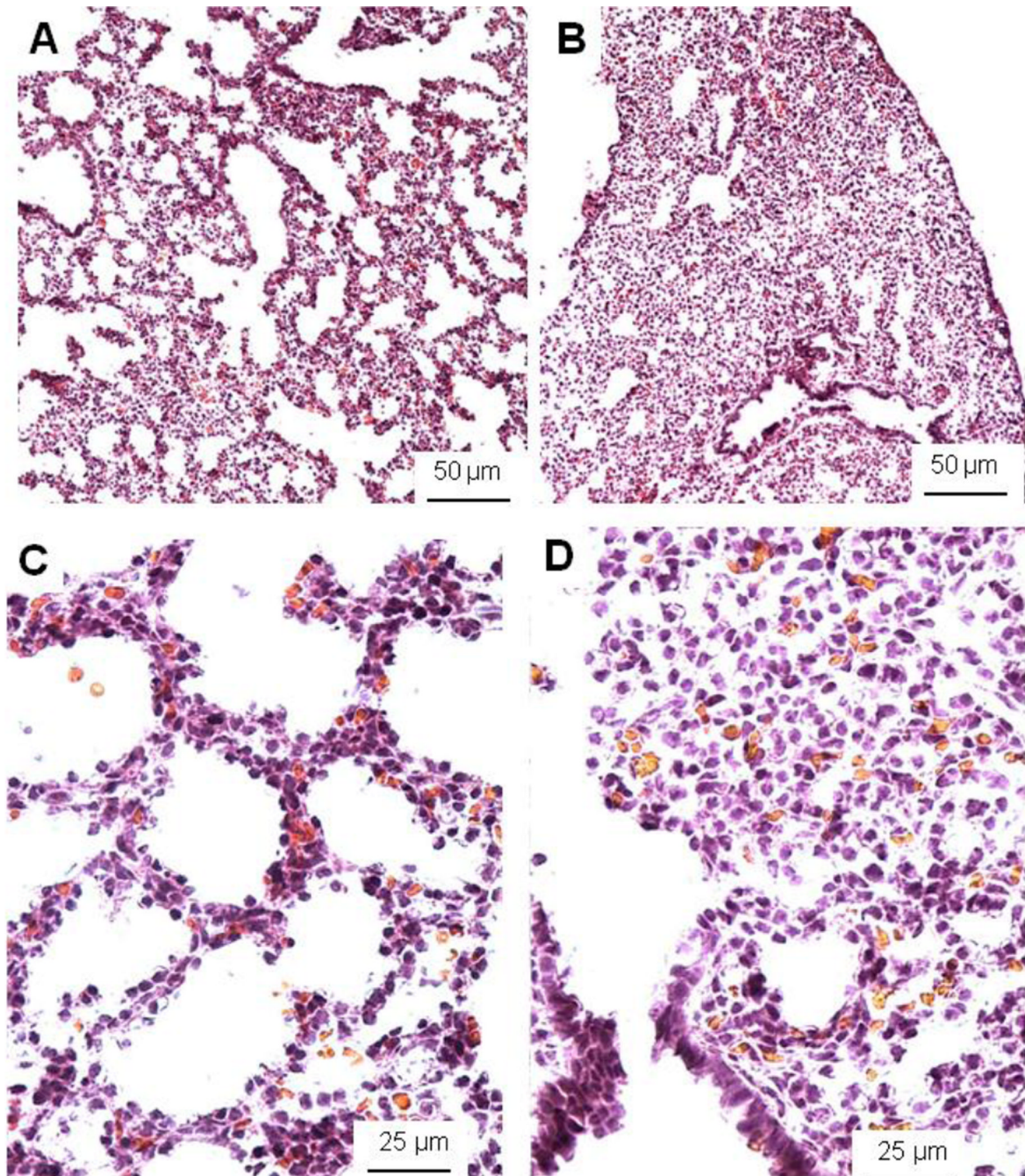
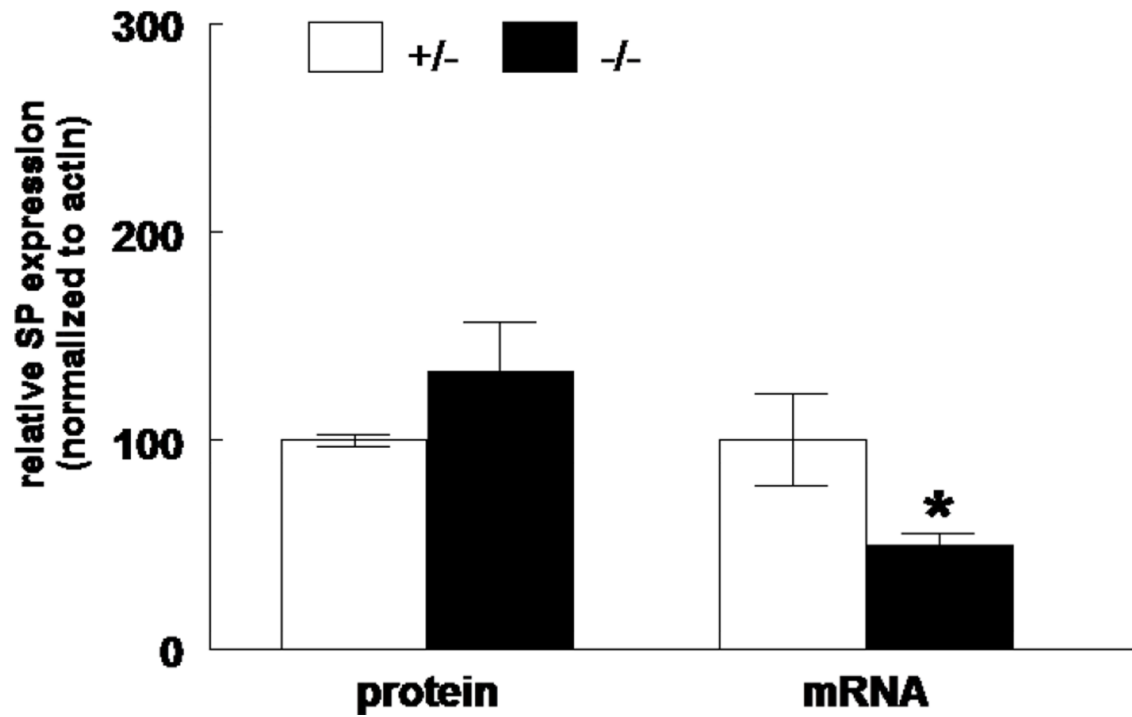
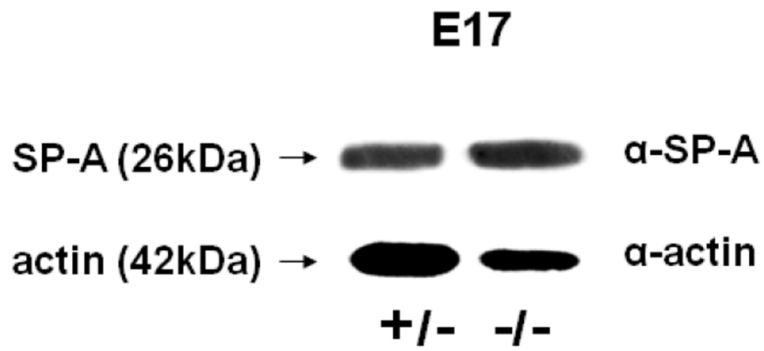
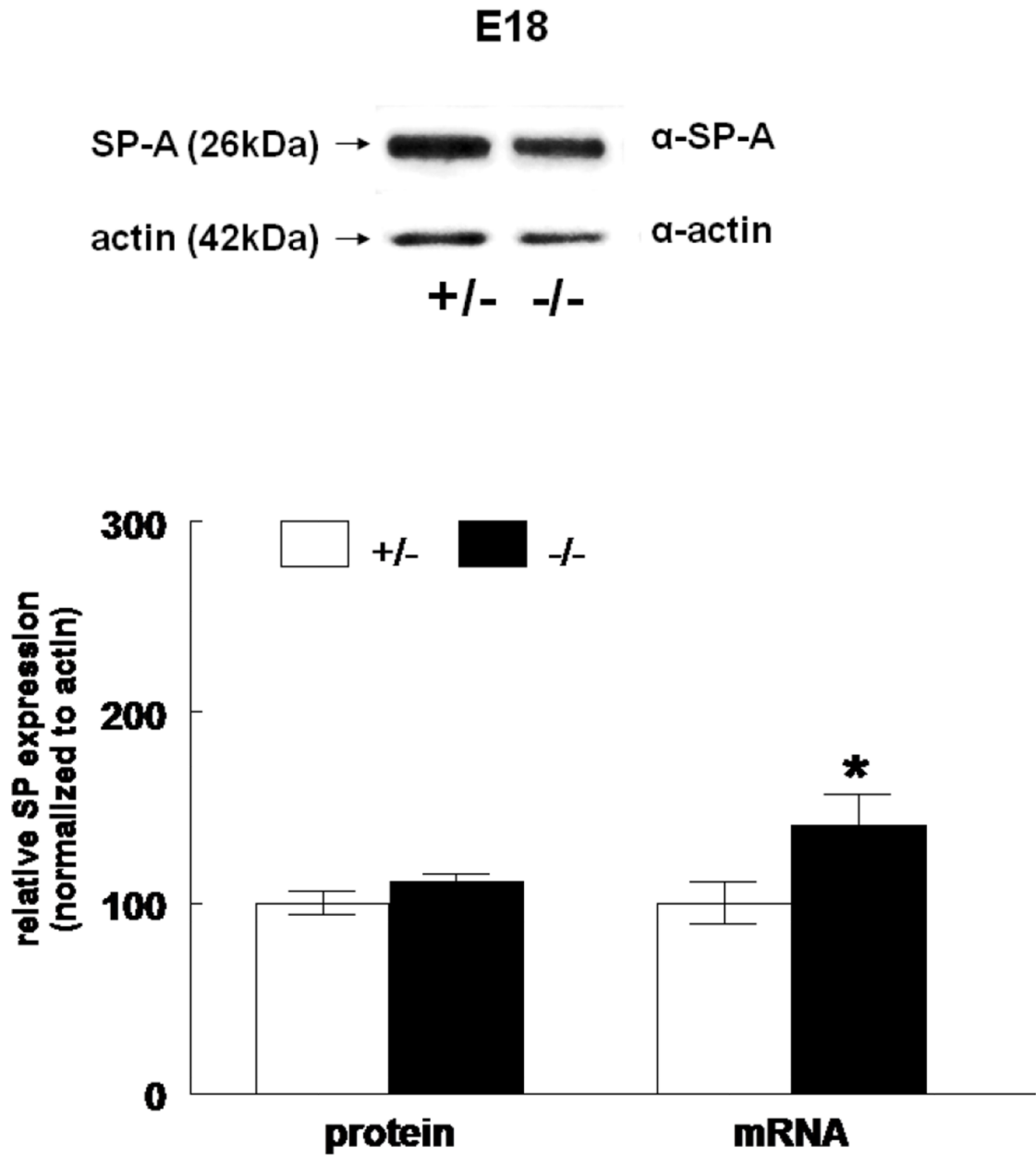


Figure 2. Histological pictures of E17 control $HER4^{heart+/-}$ (A, C) and $HER4^{heart-/-}$ (B, D) lungs. Representative light microscopic images from cryosections stained with hematoxylin and eosin. $HER4^{heart-/-}$ (B) lungs have fewer transitory ducts and saccules compared to $HER4^{heart+/-}$ control lungs (A). A higher resolution shows more epithelial cells surrounding the air spaces in control lungs (C). $HER4^{heart-/-}$ (D) lungs have less sacculi and show accumulation of tissue containing mesenchyme cells. Morphometric evaluations revealed an increased volume density of the septal tissue and a decreased volume density of the airspace in $HER4^{heart-/-}$ lungs.

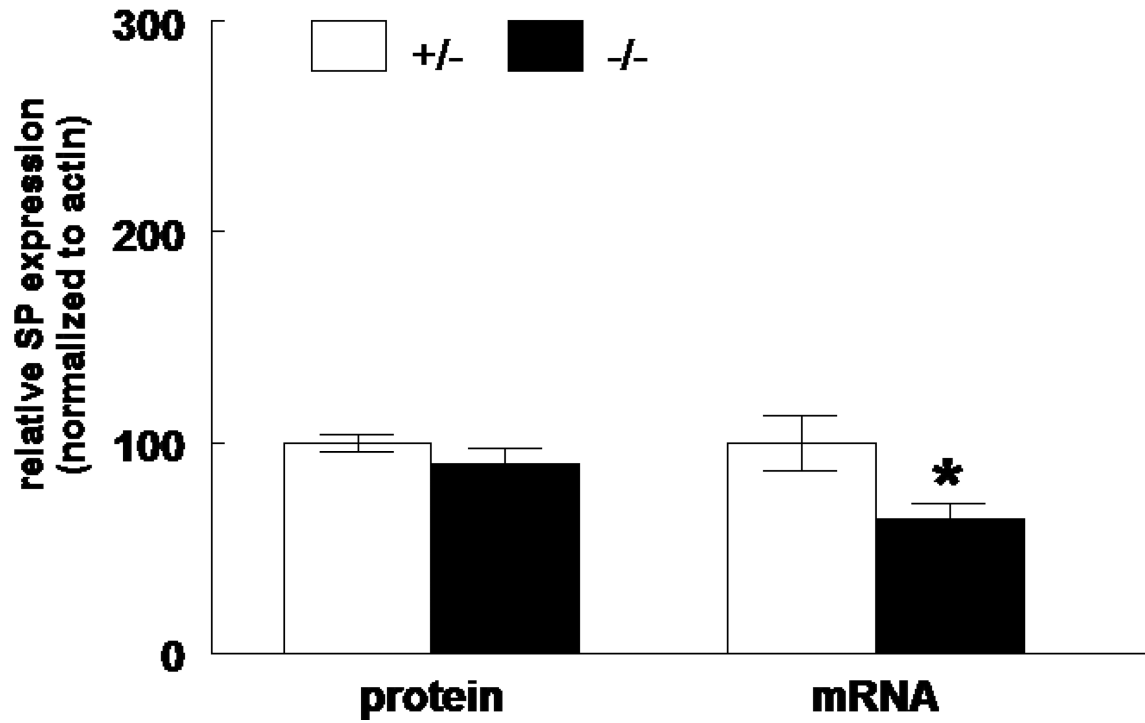
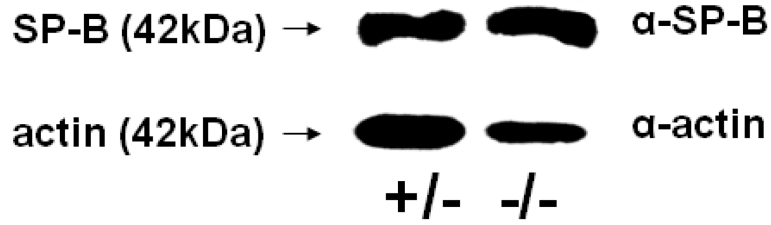
A

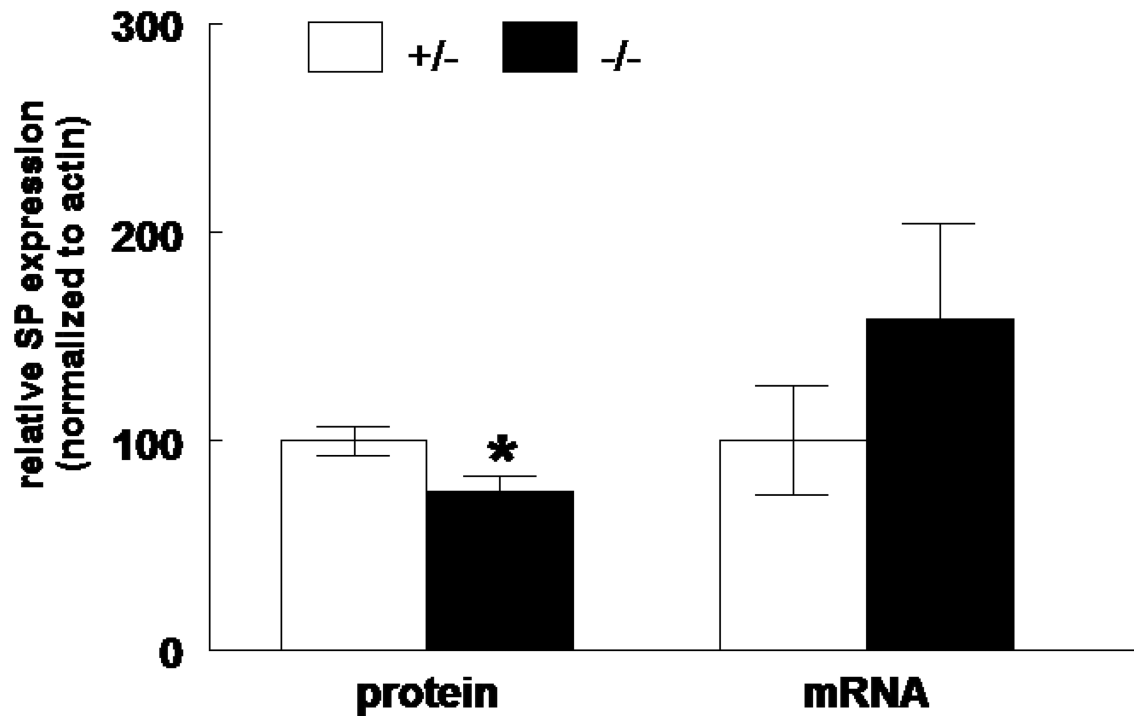
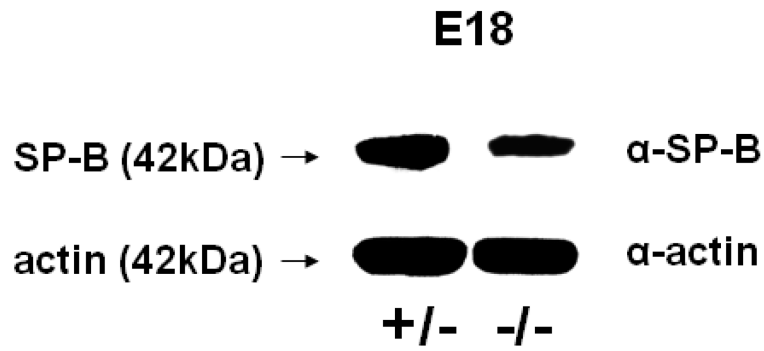


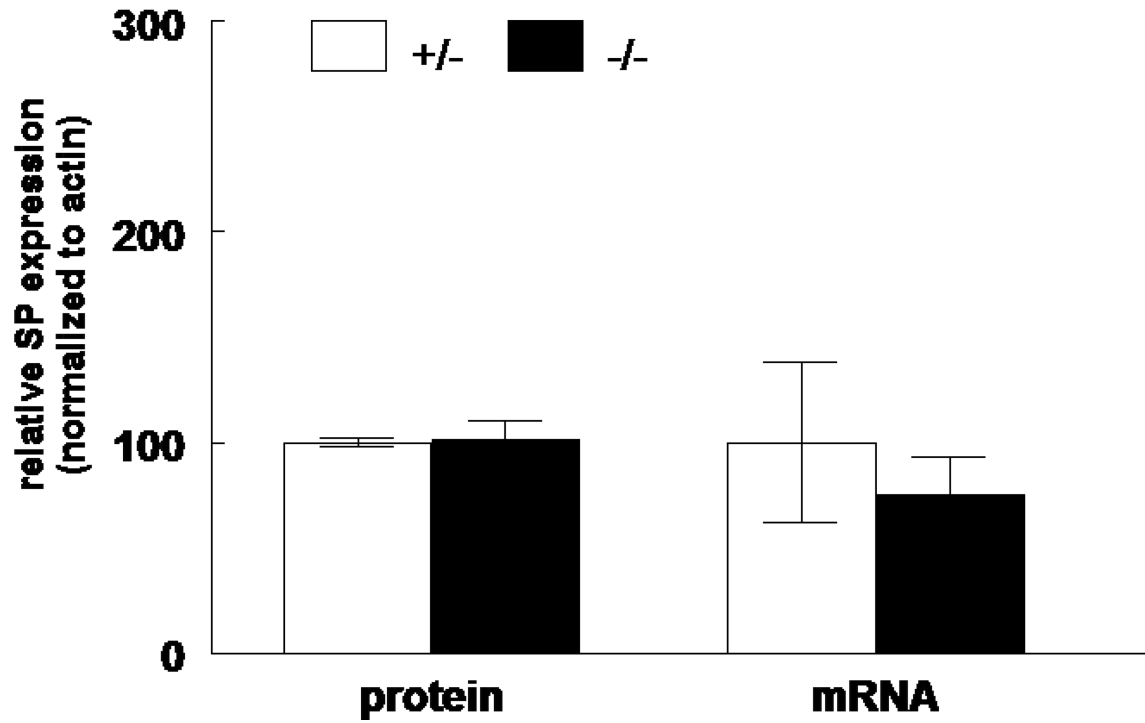
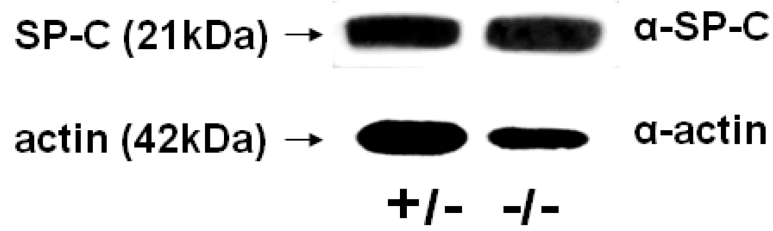
B

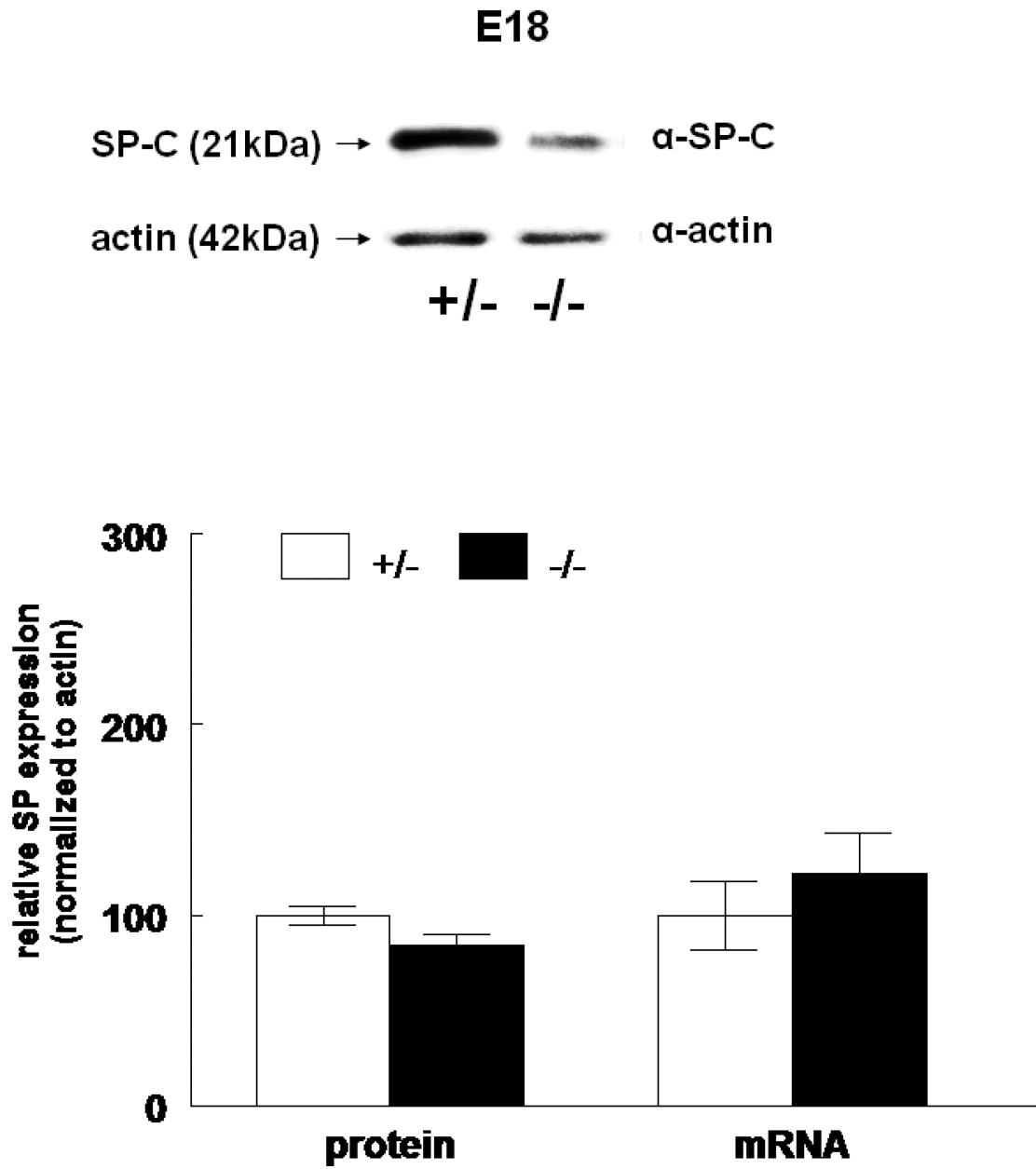
C

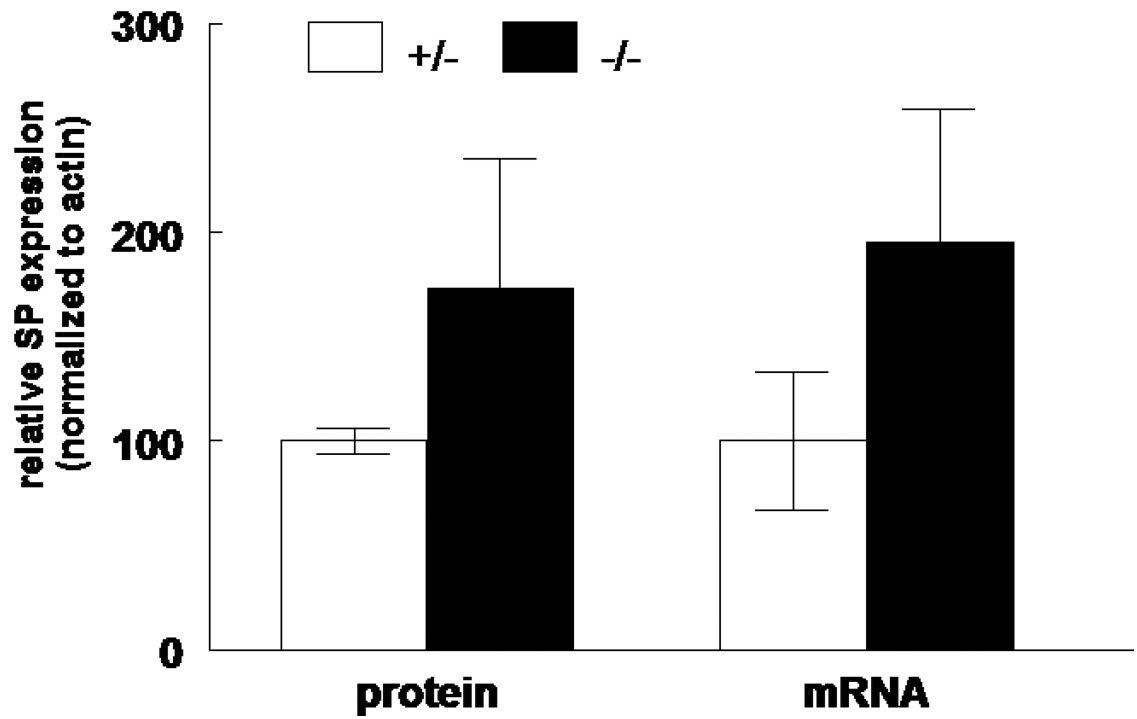
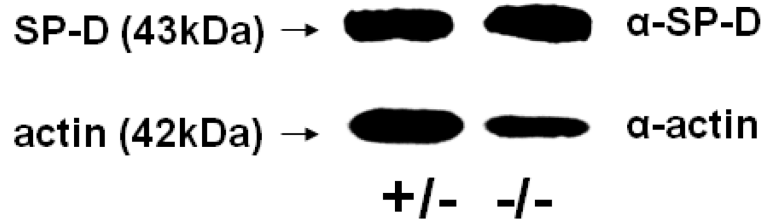
E17



D

E**E17**

F

G**E17**

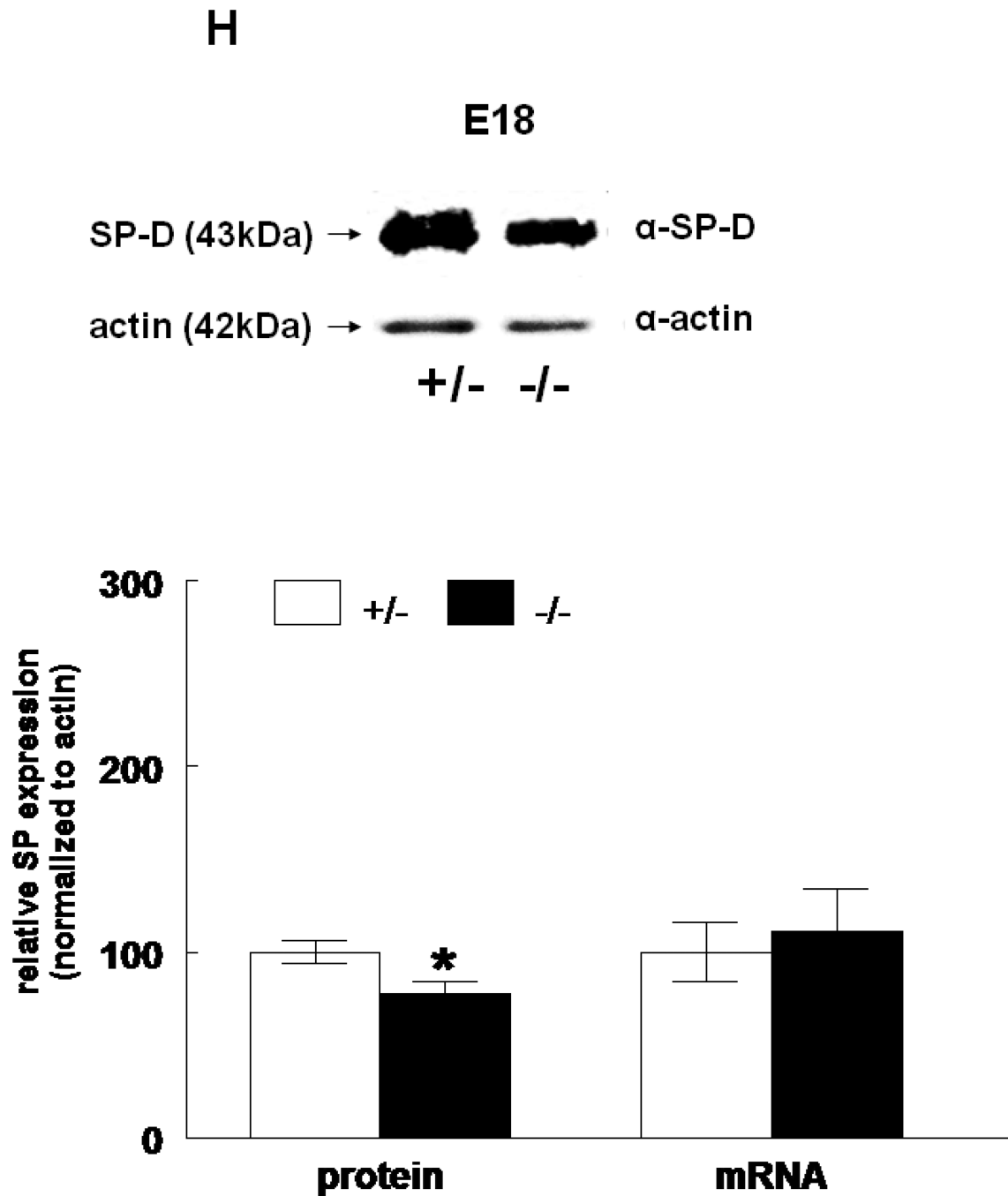


Figure 3. SP expression. SP-A, SP-B, SP-C, SP-C, and SP-D protein expression in E17 (A, C, E, G, respectively) and E18 (B, D, F, H, respectively) lungs. Representative Western blot from $HER4^{heart+/+}$ (left) and $HER4^{heart-/-}$ (right) lung homogenates. Quantification of protein (left) and mRNA (right) expression in lung homogenates from $HER4^{heart+/+}$ (white bars) and $HER4^{heart-/-}$ (black bars) transgenic mice. Values are presented as mean \pm SEM, N= 4*: P<0.05.

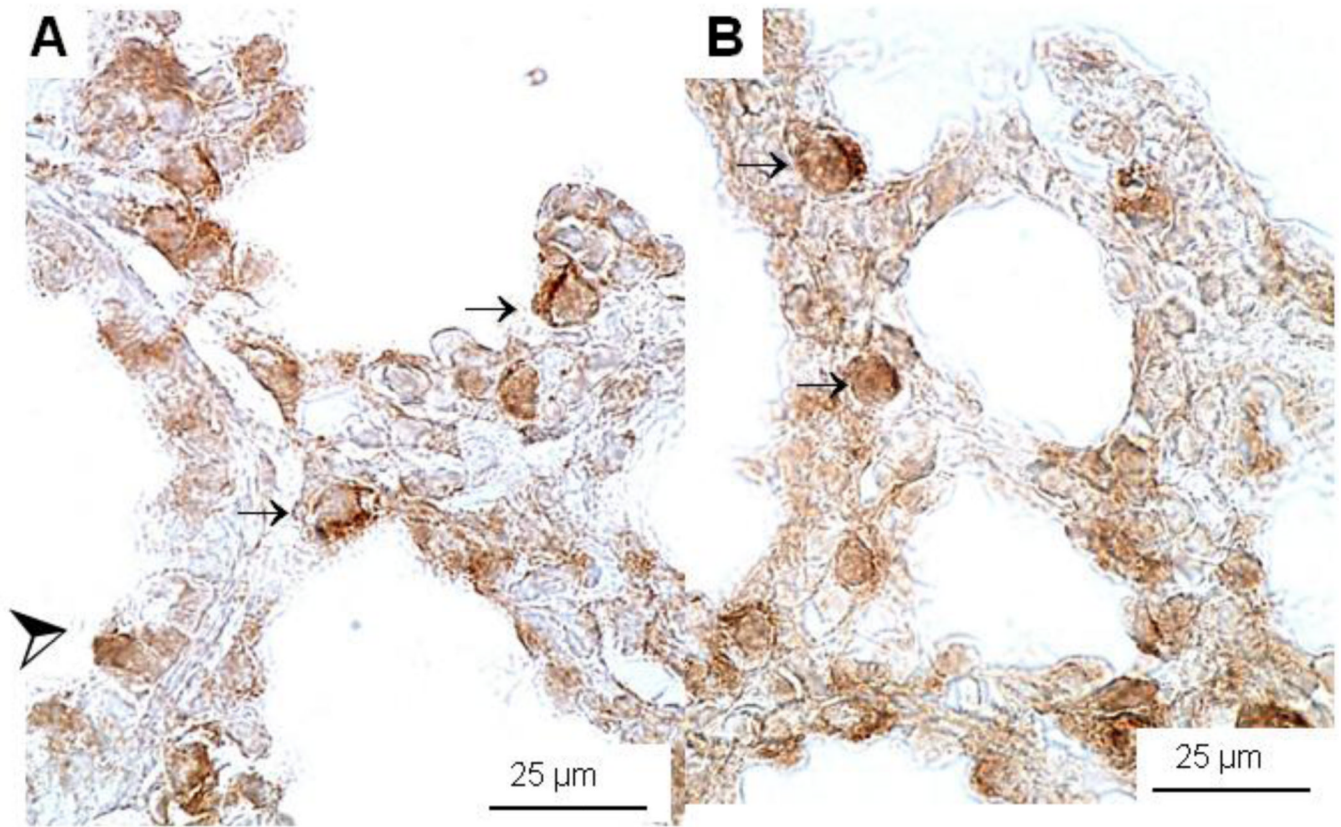


Figure 4. Immunohistochemistry of SP-B protein expression in E18 control HER4^{heart+/-} (A) and HER4^{heart-/-} (B) fetal lung. Representative images of lung sections from HER4^{heart-/-} lungs (B) compared with HER4^{heart+/-} control lungs (A). Dark brown staining is seen in SP-B-positive cells which include type II epithelial (small arrows) and Clara cells (large arrow head).

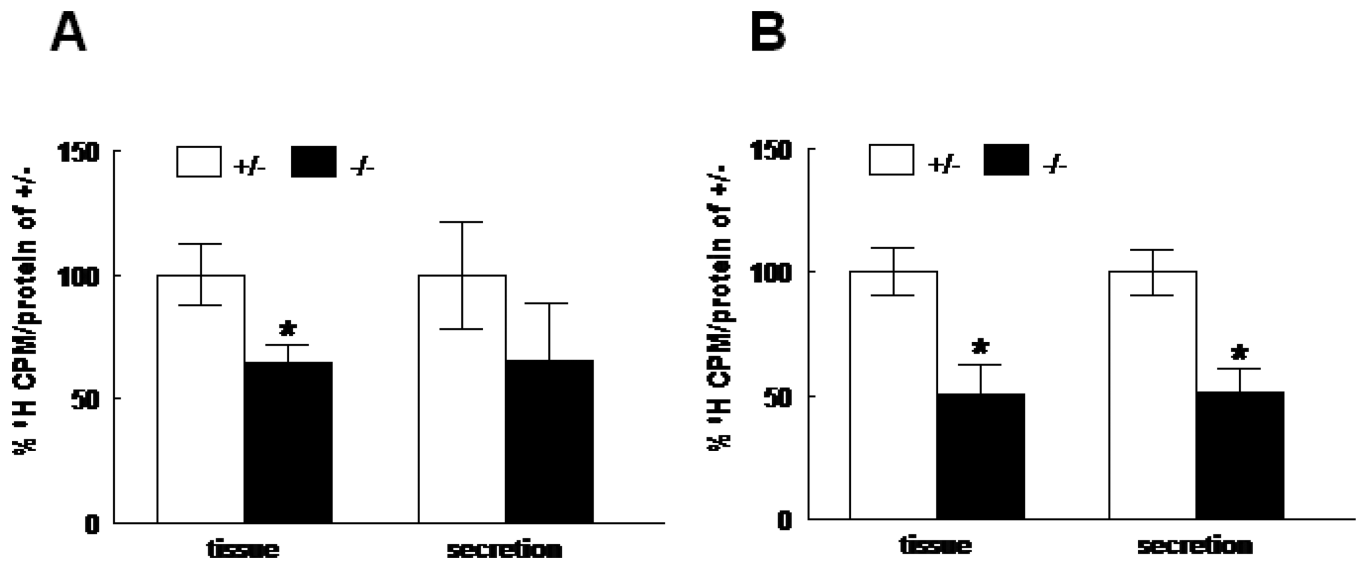
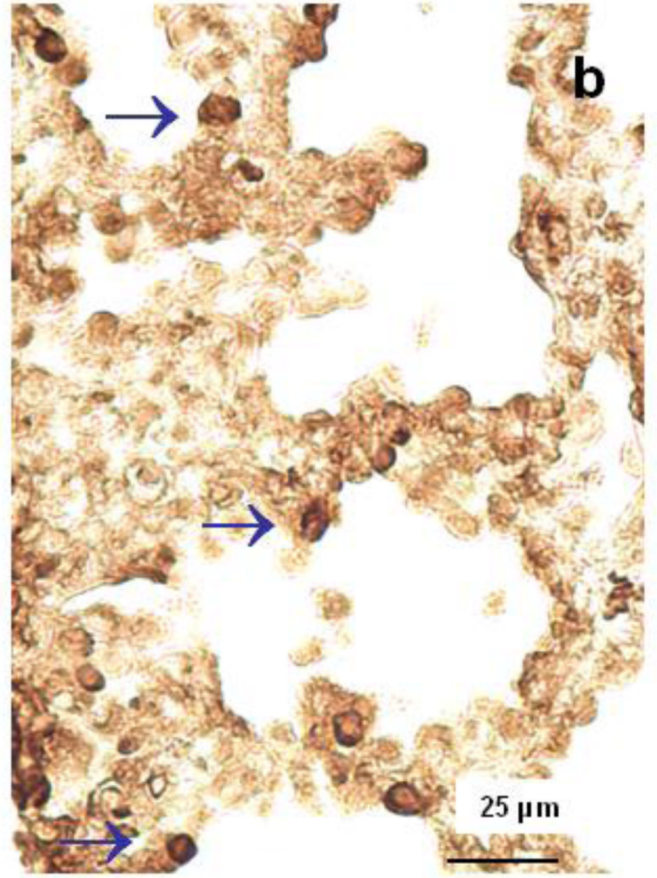
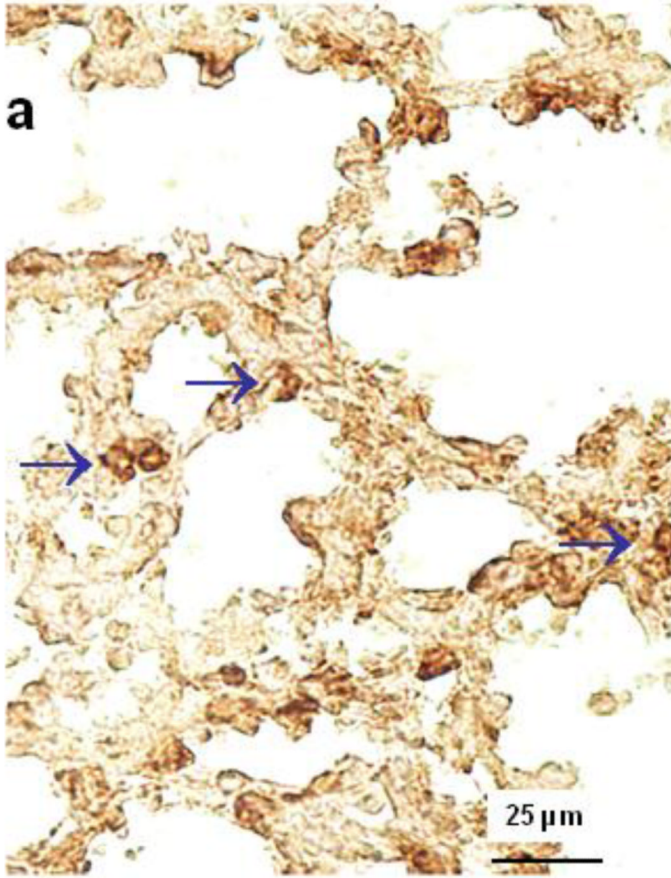


Figure 5. DSPC synthesis (left group) and secretion (right group) in E17 (A) and E18 (B) fetal lung homogenates from HER4^{heart}+/- (white bars) and HER4^{heart}-/- (black bars) transgenic mice. Values are presented as mean \pm SEM, N=4–14, *: P<0.05.

A



B

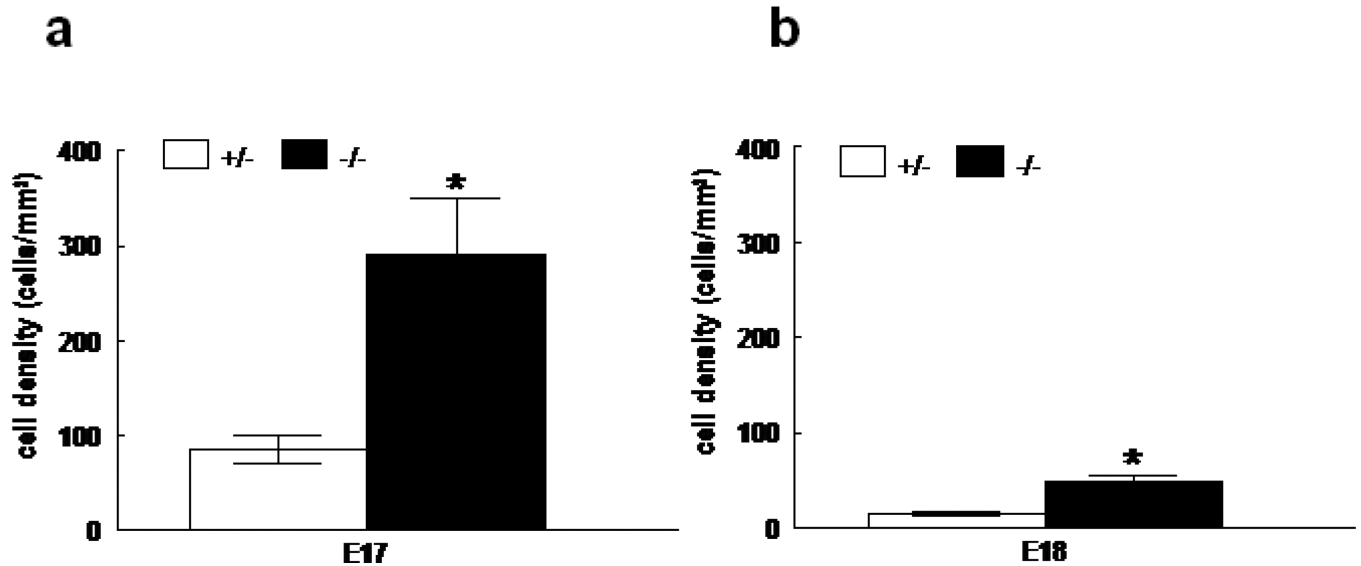


Figure 6.

A: Representative immunohistochemical images of CD11b expression in E18 control $HER4^{heart+/-}$ (a) and $HER4^{heart-/-}$ (b) fetal lung sections. Arrows indicate CD11b-positive cells, which are more frequently seen in $HER4^{heart-/-}$ lungs. B: Quantification of cell density (cells/mm²) of CD11b positive cells in E17 (a) and E18 (b) fetal $HER4^{heart-/-}$ lungs (black bars) compared with $HER4^{heart+/-}$ control lungs (white bars). Values are presented as mean \pm SEM, N= 7, *: $P < 0.05$.

Table 1

Morphometric parameters in the lungs of E18 HER4^{heart-/-} mice compared with control HER4^{heart+/-} mice.

Morphometric parameters	% of litter-specific control	P value
Volume density of parenchyma	100.44±0.39	0.35
Volume density of non parenchyma	92.85±8.84	0.22
Thickness of saccular septa	94.39±2.6	0.10
Volume density of saccular septa	98.46±2.42	0.76
Volume density of saccular space	95.73±3.02	0.46
Surface density of saccules	105.01±2.83	0.23
Size of alveolar saccules	91.78±2.92	0.04*
Volume density of ductal space	104.39±6.0	0.70
Size of alveolar ducts	95.18±3.83	0.45
Volume density of ductal septa	108.51±4.67	0.17
Thickness of alveolar ductal septa	102.11±3.27	0.68

Data presented as mean (%)±SEM.

* p<0.05

Table 2

Morphometric parameters in the lungs of E17 HER4^{heart-/-} mice compared with control HER4^{heart+/-} mice.

Morphometric parameters	% of family specific control	P value
Thickness of septal tissue	122.74±6.58	0.016*
Volume density of septal tissue	122.23±3.50	< 0.001*
Volume density of airspace	73.71±3.92	< 0.001*
Surface density saccules/canalicules	104.01±4.42	0.91
Size saccules/canalicules	71.77±3.70	< 0.001*

Data presented as mean (%)±SEM.

* p<0.05